1. OSO-7 SPECTROHELIOGRAPH MECHANISMS

Donald N. Matteo

General Electric Company - Space Division
Valley Forge, Pa.

SUMMARY

The OSO-7 Orbiting Solar Observatory was launched on September 29, 1971. One of the two main sun pointing instruments aboard was the Goddard Space Flight Center Spectroheliograph for monitoring extreme ultraviolet (EUV) and X-ray radiation from the sun. The instrument, which was designed, built and tested by General Electric Company for NASA-GSFC, has been operating successfully in orbit for approximately two years.

The design solution to each of the mechanism tasks is described. Also described are certain developmental problems and their solutions which led to the ultimate mission success.

INTRODUCTION

Orbiting Solar Observatory-H (redesignated OSO-7 upon successful orbit injection) is an earth orbiting spacecraft which is the platform for several sun observing instruments. The spacecraft contains two experiments which are precisely pointed at the sun by a spacecraft provided orientation system. The EUV and X-ray spectroheliograph is the "right-hand" member of this pair of sun pointing instruments. Its position and relationship to the spacecraft and other scientific instruments are shown in Figure 1.

The instrument consists of five separate scientific experiments. These are:

- o Extreme Ultraviolet (EUV) Spectroheliograph
- o H-Alpha Spectroheliograph
- o Longwave (LW) X-Ray Spectroheliograph
- o Shortwave (SW) X-Ray Spectroheliograph
- o X-Ray Polarimeter

The locations of these five experiments within the instruments are shown in Figure 2. Figure 3 is a photograph of the instrument showing the same general arrangement as Figure 2.

EUV Spectroheliograph

The EUV spectroheliograph is designed to obtain spectroheliograms in the EUV region between 170 and 400 Å. The experiment consists of an imaging system (grazing incidence telescope), a variable aperture mechanism located at the focal plane of the telescope, a grating, and a carriage mechanism which scans the first order diffracted component from the grating, the scan being made along the spectrometer's focal curve. The variable aperture mechanism permits the selection of four different on-axis apertures and also provides the capability to scan the solar diameter when the instrument is center-sun pointing. The carriage mechanism contains three magnetic electron multipliers (MEM), a set of two selectable exit slits for each MEM, and associated drive motors and electronics. This arrangement permits three lines of radiation to be selected and observed at one time. Items of interest to the mechanism designer in this experiment are:

- o The carriage scan mechanism,
- o The variable aperture mechanism,
- o The exit slit selection mechanism.

Longwave X-Ray Spectroheliograph

The Longwave X-ray experiment provides spectroheliograms in selected spectral bands between 7.9 Å and 16 Å. The experiment consists of a collimator, a filter wheel mechanism, a double chambered proportional counter, and associated electronics. The filter wheel has 6 positions; five containing filter pairs and one "open" position which is used for calibration. Each filter pair consists of two side-by-side filters, each of which is common to only one of the two chambers of the proportional counter. With a filter pair placed in front of the proportional counter, it is possible to measure radiation in a very narrow spectral band by obtaining the difference in the outputs of the two proportional counter chambers.

Shortwave X-Ray Spectroheliograph

The Shortwave X-Ray experiment provides spectroheliograms in selected bands between 1.7 Å and 8 Å and operates in the same manner as the Longwave X-Ray system.

The filter wheel mechanism, which provides the filter selection functions for both the LW and SW X-Ray spectroheliographs, is a mechanism of interest which is described in this paper.

H-Alpha Spectroheliograph and X-Ray Polarimeter

Both of these experiments are passive from a mechanisms standpoint (after initial precision alignments are completed) and are not discussed in detail herein.

EUV EXPERIMENT MECHANISMS

EUV Variable Aperture Mechanism

The entrance aperture of the EUV Spectroheliograph is located at the focal surface of the EUV grazing incidence telescope.

The entrance aperture determines the size and location (relative to the solar disc image) of the image element entering the EUV Spectroheliogram. It thus contributes to the spectral resolution and the scanning capability of the instrument. The variable aperture assembly is required to:

- Selectively admit to the spectroheliograph image elements of 10 x 20 arc-seconds, 20 x 20 arc-seconds, 40 x 20 arc-seconds, 20 x 60 arc-seconds (on-axis of the EUV telescope).
- Provide for the scan of a 20 x 20 arc-second image element across the diameter of the solar disk in 90 equal steps.
- During scan, the aperture slit must track the curved surface of focus of the telescope in the direction perpendicular to the scan along the line of sight of the telescope.
- The mechanism must include an indexing feature to permit return of the image element to the optic axis upon ground command.

The variable aperture mechanism consists of a 20 arc-second wide (approximately 0.08 mm at focus of telescope) fixed slit located normal to the instrument baseplate and to the incoming radiation, and of a rotating slit assembly located just in front of the fixed slit. The rotating slit limits the height of the fixed slit to 10, 20, 40, or 60 arc-seconds on-axis and also scans across the solar disc along the fixed slit with a 20 arc-second wide aperture as a function of rotary position. The rotating assembly is driven by a stepper motor and gear reduction unit. Two microswitches provide position indication of the rotary assembly and advance the position to a fixed reference position. Figure 4 shows this arrangement.

Fixed Slit. The fixed slit is bonded to the entrance slit mounting base. The slit is fabricated by electroplating nickel on a 0.00762 cm thick electrolytic copper substrate to a thickness of 0.000762 cm around the desired slit configuration (which is held to $\pm$ 0.00025 cm). The copper is then etched away in the area of the slit so that the desired slit configuration is formed by the nickel plating. This technique is used for all the slits in the instrument, including the rotating slit and the EUV exit slits.

Rotating Slit Assembly. The rotating slit assembly (which is mounted directly on the motor/gearhead output shaft) consists of the four central aperture slits and a single spiral slit. The central aperture slits are of constant radius from the center of rotation so as to always be on the optical centerline. They occupy approximately equal arc segments in 180 degrees of the disc. The blank space between the slits is bridged by an off-axis slit of larger radius so that a failure of the rotating slit drive cannot block the incoming radiation no matter what angular position the rotating slit assembly is in should a failure occur.

The spiral slit occupies the remaining 180 degrees of the disc. The radial distance of the spiral varies such that the spiral scans the diameter of the solar disc as the slit is rotated. When this arrangement of spiral slit rotating in front of a straight fixed slit was first conceived, the apertures were thought of as slits in simple flat foils arranged normal to the optical axis. However, upon more detailed investigation it was realized that the telescope focal surface was not a plane, but rather a body of revolution above the optical axis which approximated a portion of an ellipsoid. See Figure 5. Since the entrance aperture is required to be in or near the telescope focal surface, this development threatened to greatly complicate entrance aperture mechanism. After several complex design solutions were considered, however, the simple technique of mounting the spiral slit on a surface inclined to the axis of rotation was discovered to generate the required along-axis motion of the aperture as a function of off-axis scan position. As the disc rotates the axial position of that portion of the slit which defines the image element varies. By properly positioning the spiral slit on the inclined rotating member, that axial position can be made to be of longest focal length when the image element is on the center of the solar disc (optical axis) and to move to shorter focal lengths as the image element moves to either edge of the solar disc. Selecting the inclination angle controls the rate of axial travel as a function of off-axis scan. The actual angle used was 12°28' from normal to optical axis in order to scan the profile shown in Figure 5.

Drive for the rotating slit assembly is provided by 13 VDC, size 8, 90° stepper motor driving a 60.75 to 1 ratio gearhead. Lubrication technique was dry film throughout motor/gearhead. All gearhead bearings and gears were lubricated with Lubeco 905. Each individual gear and

bearing element was individually inspected and lubricated prior to assembly. The gearhead bearings were lubricated on their races and the inner surfaces of their two piece ribbon retainers. All gearhead bearings were run-in individually and torque tested prior to assembly. The motor bearings were lubricated by means of an MoS_2 bearing ball retainer. They were torque tested and run-in at assembly. Each motor/gearhead set was green-run for 100 hours in a vacuum at nominal torque and speed; then torn down, inspected and re-assembled. This same technique was used for all motor/gearhead combinations in the instrument (including EUV carriage, EUV exit slit section mechanism, and X-Ray filter wheels. While the lubrication/run-in/test procedure was rigorous, the excellent performance in orbit justifies the effort expended.

The rotating portion of the variable aperture assembly was balanced about its center of rotation (by fine ballasting) and no launch lock mechanism was used.

A thermal shield was provided just forward of the rotating disc assembly. This shield intercepts radiation from those portions of the solar image which are not to be scanned in order to minimize thermal effects on the aperture mechanism.

EUV Carriage Scan Mechanism

The carriage assembly shown in Figure 6 is a machined beryllium frame containing the three Bendix magnetic electron multiplier detectors, six spectrometer exit slits positioned on the spectrometer focal circle, the movable mask to select the desired group of three exit slits, the two microswitches for selecting the exit slit mask position, and the motor/gearhead drive for the mask. The carriage is movable along the focal circle to cover the wavelength range of 170 Å to 400 Å in approximately 0.07 Å steps. At one unique position the six exit slits are aligned with six selected EUV lines, three of which can be viewed simultaneously by each of the three detectors as selected by positioning the mask.

Carriage Drive. The carriage is supported on a track fixed to the instrument base and curved to the focal circle radius (50 cm.). A recirculating ball bearing with the balls riding in "V" groove races in the track and carriage provides low friction and stiff support for the carriage motion. The "V" groove is machined into stainless steel inserts in the beryllium track and carriage. The carriage is driven by a motor/gearhead assembly fixed to the instrument baseplate with the output pinion driving a curved stainless steel rack on the carriage. The gearhead ratio and the pinion size are such that for each 90-degree step of the motor, the carriage travels a linear distance of 0.0028 cm. or approximately 0.07 Å. This compares to a specified maximum of 0.1 Å per step. The control logic provides for three separate speeds of travel, 6.25, 12.5, or

50 steps per second. At the longwave and shortwave limit of its travel, the carriage actuates separate microswitches which give an indication to the control logic that the limit has been reached. The logic reverses the direction of travel and, when so commanded, stops the travel. Whenever a specific carriage position is to be duplicated, it is approached from the same direction as first achieved by counting motor pulses from a reference position. In this way, gearhead backlash is trimmed out and carriage positions are duplicated within one motor step. The motor/gearhead combination is the same type as that described in the section on the variable aperture mechanism except that the gearhead ratio is 305.35 to 1.

The motor/gearhead assembly, the rack and pinion, the carriage bearing races, and the ball return slots are lubricated with the same solid film lubricant system as previously described.

Exit Slit Assembly. The six exit slits are precisely positioned on a single exit slit foil by the plating and etching process described previously. The foil is then mounted to a frame and the assembly is attached to the carriage. Particular care is taken in mounting the foil to the frame to maintain the slit leading and trailing edges in the same plane. Because of the shallow angle at which that the radiation passes through the slit, any out of plane condition of the two edges would appear to be a change in width of the slit, thus affecting the spectral resolution. The spacing between the six slits is accurately held so that the six selected spectral lines appear simultaneously at the same carriage position. Because slits are tangent to the Rowland circle, their width is such that the projected width, in a plane perpendicular to the incident radiation, is 85 μm. Spectral width measurements show that the effective width is uniform within 0.1Å from slit to slit.

Flexprints. The electrical connection between the instrument electrical system and the movable carriage is made through two flexprints. One flexprint contains the two high voltage conductors and the second contains 21 low voltage conductors. The conductors are etched copper ribbons between Kapton substrates and an external coating of Teflon. The thicknesses of the copper conductors are 0.00686 cm for the low voltage flexprint and 0.01372 cm for the high voltage flexprint. The thickness of the Kapton is 0.005 cm in both cases.

The original thickness of the low voltage flexprint was 0.01372 cm. However, it was determined by life tests that this thickness was unsuitable for the bend configuration and flexing modes of the low voltage flexprint. The thickness was changed to 0.00686 cm and subsequent life tests show no failures after 43,000 cycles.

The high voltage flexprint with the 0.01372 cm thick conductors was life tested and withstood 41,000 cycles before failure. Forty-one thousand cycles represents a safety factor of approximately 4 based on the expected one-year operational mode of the instrument and was considered adequate. Actual number of flexure cycles logged in orbit as of June 1973 was 15,200

without failure. This is an actual rate of just over 9000 per year and shows the decision that the demonstrated life was adequate.

Launch Lock. The launch lock is a pyrotechnic operated device which secures the movable carriage to the track during the application of the vibration and acceleration loads of the launch environment. The launch lock is fired upon command after orbit has been achieved and spacecraft separation has occurred.

The launch lock housing is mounted externally on the instrument baseplate. A retractable pin projects through the baseplate into a close fitting hole in the carriage assembly. The locking pin is loaded by a combination torsion and compression spring. The torsion holds the pin in the locked position in a detent in the housing. The pin is rotated against this torsion load and out of the detent by dual pyrotechnically actuated pistons. The compression in the spring then retracts the pin from the carriage. The dual pistons are provided for redundancy. Both pistons are actuated by the one firing command. Each piston meets the requirements of 1 ampere, no fire, 3-1/2 amperes, all fire. Actuation of a single piston is adequate to release the locking mechanism. An advantage of this arrangement is that the locking pin can be manually engaged and disengaged by using a screw driver whether the pyrotechnic actuators are installed.

EUV Exit Slit Selection Mechanism

It is a requirement on the EUV system that there be a single position of the carriage assembly where six specific EUV lines be "visible" to the electron multipliers and that either of two groups of three of these lines each be selectable for detection by ground command, without carriage motion. As described above, the exit slits are positioned such that each of these EUV lines will pass through one of the six exit slits when the carriage is in the proper position along the track.

In order to select between the two groups of three lines, an exit slit mask is provided. This mask is positioned immediately in front of the exit slits and is configured such that it will block illumination from entering three exit slits while passing illumination to the other three exit slits. This mask travels in "V" grooves. As is the case with the carriage track, the 440C stainless steel balls roll on a 440C stainless steel "V" groove.

The mask is shuttled from one end of the track to the other by ground command and is stopped by the actuation of a microswitch at each travel extreme. At one end of its travel, the mask uncovers one group of three slits and, at the opposite end, the mask uncovers the other three slits while covering the original group. The slits are positioned in pairs such that energy entering either slit of a given pair enters one of the three detectors (electron multipliers). The mask is configured to uncover one slit of each of the three pairs at each end of its travel.

Mask drive is provided by a motor/gearhead unit which is mounted on and rides with the carriage. The output of the 48 to 1 ratio gearhead is delivered to the mask by means of an eccentric arm acting on a slot in the mask assembly. The output of the eccentric is delivered to the mask by means of ball bearing with its outer ring rolling in the slot. A 180 degree rotation of the eccentric arm (gearhead output shaft) results in mask travel from one end of its track to the other. In this way, extreme accuracy of output shaft position (as affected by backlash) is not required since mask position accuracy is a function of the difference in cosines of small angles.

The motor, gearhead, "V" groove track, and mask slot are lubricated by the same MoS_2 dry film system as described previously.

LW&SW X-RAY MECHANISMS

Both the longwave and the shortwave X-ray experiment designs consist of a collimator to provide the spatial selectivity and side lobe suppression, a set of five balanced filter pairs to provide the spectral bands of interest, a double channel proportional counter, and associated electronics. The filter pairs are mounted on a 6-position filter wheel which is motor-driven so that each of the 5 filter pairs and an open position may be placed in front of the double-channel proportional counter by command. The channels in the detector are side-by-side (A&B) as are the filters (A&B) in each filter pair; therefore, the output of each channel (A or B) is a function of the filter which is placed in front of the channel.

X-Ray Filter Wheel Mechanism

The filter wheel assembly, shown in Figure 7 contains the longwave and shortwave filter wheels which rotate independently about a common pedestal to insert wavelength selective filters in the X-ray path. Each wheel has provision for mounting six such filter pairs. One filter pair position is left open to provide a position where unfiltered X-ray energy will enter the detectors (X-ray proportional counters). The proportional counters and their associated electronic amplifiers are mounted internally within the pedestal.

The filter wheel rotates on a large diameter thin cross-section bearing. A large ring gear is attached to the wheel. Each wheel is driven independently through its ring gear by a separate motor/gearhead similar to the other motor/gearheads in the instrument. The gearhead ratio is 8.476 to 1. The rotation of the wheels is controlled by two microswitches for each wheel. One microswitch engages the detents when the filter is fully in front of the proportional counter. It provides an input to the control logic to stop the wheel in this position and to advance the filter position count. The second switch is actuated once each complete revolution by a

pin projecting from the wheel. This actuation resets the telemetered filter position count.

Each wheel also contains a radioactive source which comes into view of the detector once each revolution of the wheel. The source provides a calibration level for the system.

The filter wheel bearings, ring gear and gearhead output pinion are lubricated with the same solid film lubricant system described previously.

A unique feature of this mechanism is that, as a weight and space saving technique, each filter wheel is mounted on a single, large diameter, slim cross-section bearing. This was deemed tolerable due to the balanced nature of the wheel, its light weight, and high diameter to depth ratio. No launch lock mechanism was employed in the filter wheel. This technique has worked well through vibration tests and the flight program.

PROBLEMS ENCOUNTERED

During the development of the mechanisms described herein, the following problems were encountered:

(1) Problem - Filter wheel motor/gearhead would move two steps on single step command, would slew instead of run in-synch.

Causes - High reflected inertia, voltage pulse being cut-off to motor winning at point of maximum step overshoot.

Solution - Voltage pulse increased from 15 mS to 40 mS to improve electrical detenting.

(2) Problem - EUV variable entrance aperture wheel would not stop at reference position after qualification vibration.

Cause - Reference cam deformed by impacting of microswitch actuator arm during vibration.

Solution - Recontoured cam to increase bearing area. Implemented operational change which positions wheel in rotational position where actuator arm is not in contact with cam during vibration (launch).

(3) Problem - EUV mask did not move upon command after qualification vibration.

Cause - Brinelling of beryllium "V" groove by mask support balls.

Solution - Changed "V" groove design to incorporate stainless steel insert (similar to main carriage track).

(4) Problem - EUV mask did not stop at end of travel.

Cause - Improper setting of microswitch.

Solution - Widened actuation range of microswitch.

(5) Problem - SW X-Ray filter wheel did not respond to commands.

Cause - Torque output marginal to overcome 'O'-Ring drag and ramp effect on indexing cam.

Solution - Removed 'O'-Ring (seal not required due to solid lubricant) and changed shape of indexing cam.

(6) Problem - EUV carriage launch lock did not fully retract.

Cause - Repeated firings of the same launch lock assembly raised a burr in the housing which hung-up retraction pin.

Solution - Replaced launch lock after implementing design change which chamfers corner where burr was raised.

CONCLUDING REMARKS

The author wishes to thank Dr. Werner Neupert, NASA-GSFC Principal Investigator, and Mr. Milton Kalet, NASA-GSFC Technical Officer, for their contribution to the successful development of the hardware discussed. Particular note should be made of the fact that the original concept for the EUV entrance slit mechanism was provided by GSFC in the RFP specification.

The mechanisms discussed by no means represent all of the challenges presented to the mechanical system designer by the OSO-7 spectroheliograph instrument. Such items as telescope optics mounts, beryllium structure stabilization, maintenance of precision alignments through environments, X-ray mechanical collimation, and thermal control were of great importance in achieving the precision and reliability demonstrated by the instrument in orbit. However, those items discussed are representative of fully matured, space proven hardware of the type of interest to the mechanism designer. It is hoped that some of the techniques presented will be helpful in the design of future hardware of this type.

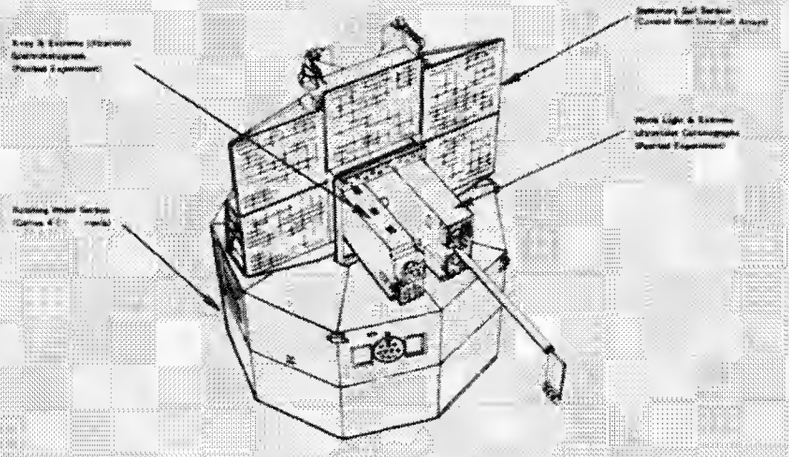

Figure 1.- Orbiting solar observatory-H.

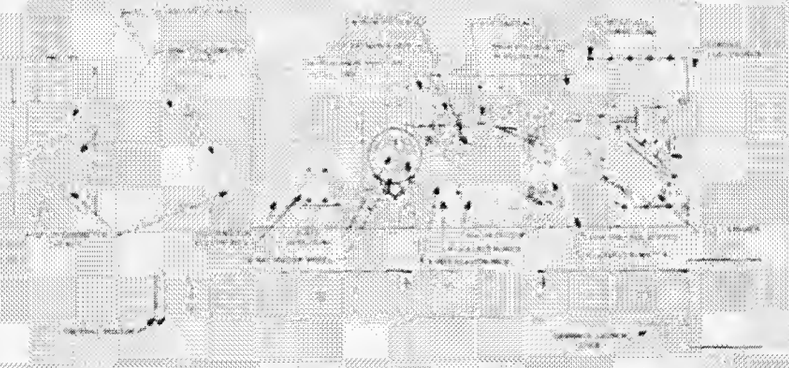

Figure 2.- OSO-H spectroheliograph general arrangement.

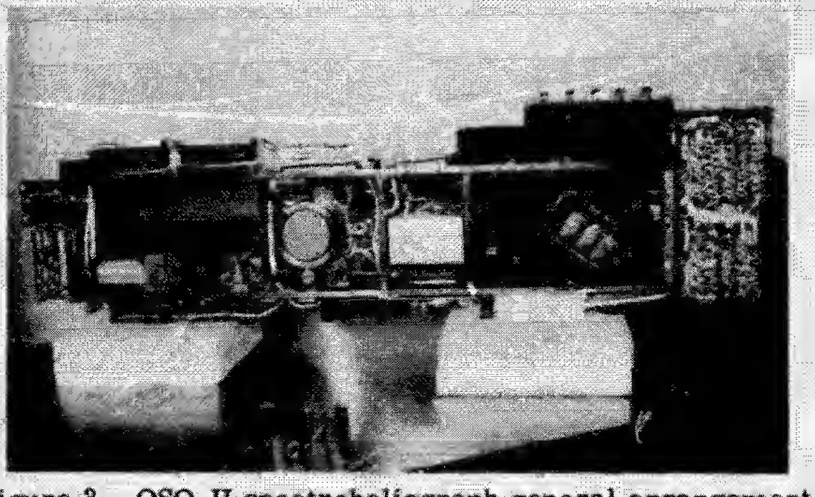

Figure 3.- OSO-II spectroheliograph general arrangement.

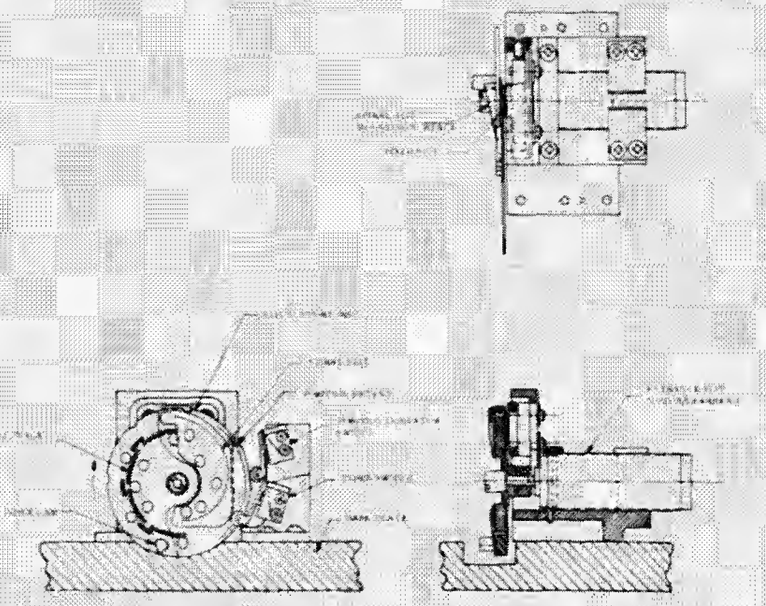

Figure 4.- EUV variable aperture mechanism.

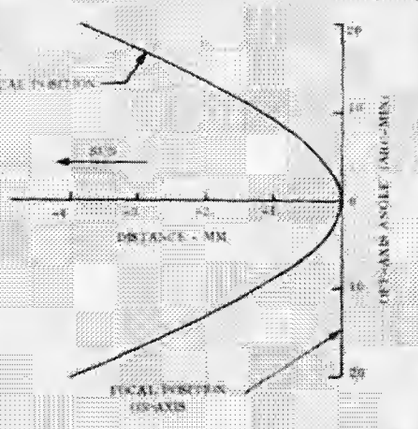

Figure 5.- Variation of curvature of focal surface with angle of off-axis radiation.

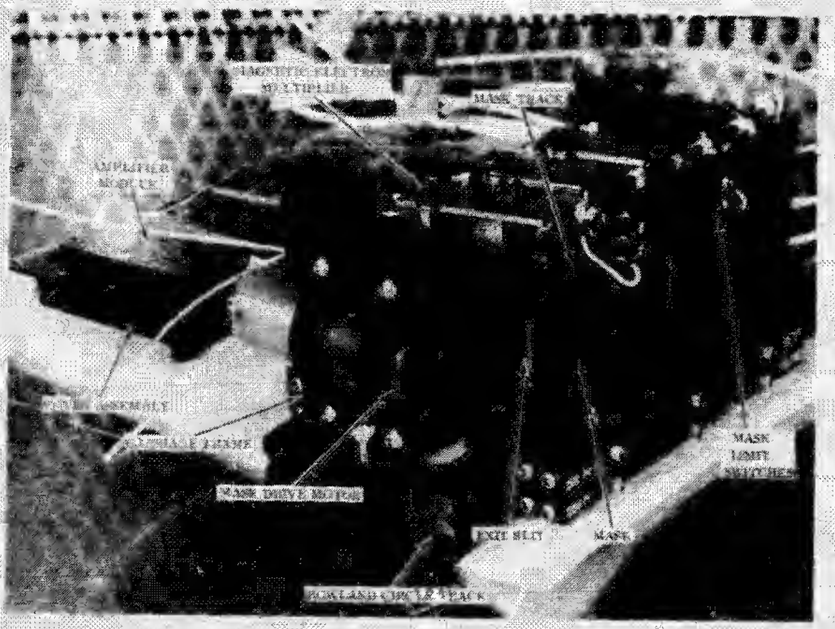

Figure 6.- EUV carriage mechanism.

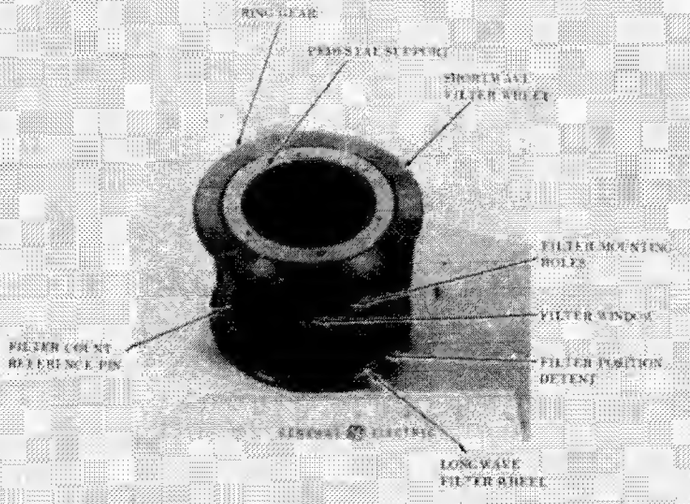

Figure 7.- X-ray filter wheel mechanism.